Unbalanced DCB-specimen

J.L. Högberg[1]
Mechanics of materials, University of Skövde, Box 408, SE-541 28, Sweden

Abstract

The Double Cantilever Beam (DCB) specimen is a common test geometry for testing of mode I fracture properties of adhesive joints. However, when unbalances are introduced to the adherends, the adhesive layer is loaded in a combination of peel (mode I) and shear (mode II). In this work the unbalanced DCB-specimen is studied by the use of the beam/adhesive layer (B/A) model, in which the adherends are considered as beams and the adhesive layer as a generalised spring media. The effect of the thickness of adhesive layer together with the effect of the geometrical and material unbalances is analysed. The result of the B/A model is compared to the continuum model through FE-simulations. Finally, an unsymmetric DCB-specimen is dimensioned for mixed mode testing of adhesive layer.

Keywords: adhesive layer; mixed mode testing; Double Cantilever Beam specimen

1. Introduction

For a symmetric DCB-specimen, i.e. a DCB consisting of two identical adherends, the adhesive layer deforms in pure mode I. The symmetric DCB-specimen is a common test geometry for measuring and studying peel or cleavage properties of adhesive joints, e.g. ASTM D 3807-79 and BS 7991:2001. However, a mode mixity can be achieved by introducing unbalances in the adherends, i.e. allowing the adherends to be made of different materials and to have different thickness. Such a specimen is denoted the unbalanced DCB-specimen. An unsymmetric DCB-specimen is a special case of an unbalanced DCB-specimen; it has adherends made of same material but different thickness.

In an adhesive joint, the adhesive layer is normally much thinner and less stiff than the adherends, and the overlap length is much larger than the thickness of the adherends, i.e. $t << t_{1,2} << L$, a common modelling technique is to treat the adherends as Euler-Benoulli beams and the adhesive layer as a generalised spring medium. This model of adhesive joints is referred to as *the beam/adhesive layer model* in the sequel (Klarbring 1991, Andersson and Stigh 2004, Högberg 2004); the B/A model for short.

Generally, in fracture mechanics, the deformation of an adhesive layer is described as a combination of three modes: peel (Mode I), in-plane shear (Mode II) and out-of-plan shear (Mode III). Through an asymptotic expansion method, Klarbring (1991) concluded that the deformation of an adhesive layer that is constrained between two relatively stiff substrates deforms in six different modes in a plane. The peel and the shear modes are the two dominating modes, which correspond to the notation mode I and II in fracture mechanics. The out-of-plane shear behaviour in mode III is similar to mode II. Thus, the simplified model of the linear elastic adhesive layer is a bi-directional spring media with two uncoupled stress-deformation relationships: the peel stress σ solely to the peel deformation w in Mode I and the shear stress τ solely to the shear deformation v in Mode II, cf. Fig. 1.

As shown by Högberg (2004), the governing equations for an arbitrarily end-loaded single-layer adhesive joint result in two coupled differential equations for the adhesive layer in terms of its peel and shear deformation, w and v, respectively

$$\begin{cases} w^{IV}(x) - Av'(x) + Bw(x) = 0 \\ v'''(x) - Cv'(x) + Dw(x) = 0 \end{cases} \qquad \text{(1a, b)}$$

[1]Corresponding author. Tel: +46 (0)500 448543; fax: +46 (0)500 448549;
E-mail: li.hogberg@his.se

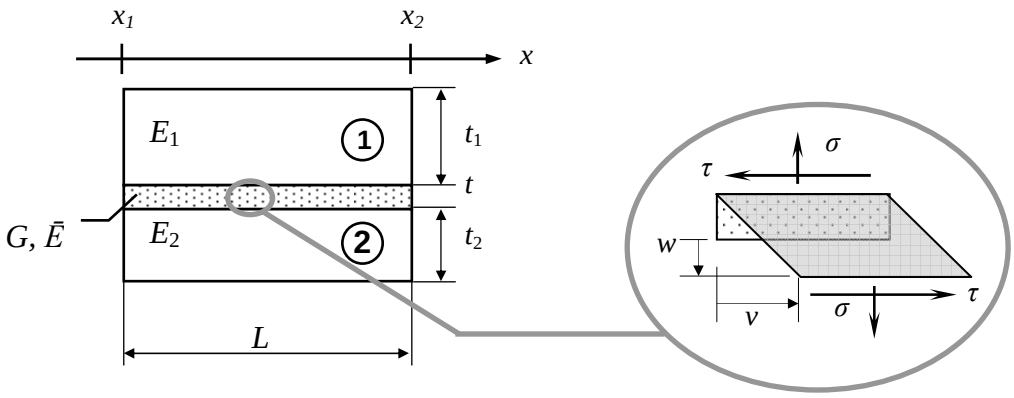

Figure 1 The dominating deformation modes of an adhesive layer are peel (mode I) and shear (mode II).

with four cross-sectional parameters

$$A=\frac{6G}{t}\left(\frac{1}{E_2t_2^2}-\frac{1}{E_1t_1^2}\right),\qquad B=\frac{12\overline{E}}{t}\left(\frac{1}{E_2t_2^3}+\frac{1}{E_1t_1^3}\right),$$
$$C=\frac{4G}{t}\left(\frac{1}{E_2t_2}+\frac{1}{E_1t_1}\right),\qquad D=\frac{6\overline{E}}{t}\left(\frac{1}{E_2t_2^2}-\frac{1}{E_1t_1^2}\right) \qquad \text{(2a, b, c, d)}$$

where $t_{1,2}$ and $E_{1,2}$ are the thicknesses and Young's modulii of the adherends, and t is the thickness of the adhesive layer. The shear modulus of the adhesive is $G = E/[2(1+\nu)]$, where E and ν are the Young's modulus and the Poisson's ratio of the adhesive, respectively. The modulus of the adhesive in peel (mode I) is given by the effective Young's modulus $\overline{E} = E(1-\nu)/[(1-2\nu)(1+\nu)]$. The seven geometrical and material parameters, $t_{1,2}$, $E_{1,2}$, t, G and $\overline{E}$, are thus replaced by the four cross-sectional parameters, A, B, C and D, which describe the geometrical and material properties of the cross section of a typical single-layer adhesive joint. These parameters are independent of the overlap length L and the joint width b.

Macroscopically, the ends of the overlap area for a single-layer adhesive joint can be considered as crack tips. The length of the un-joined part of the adherends are then considered as the crack length, a, cf. Fig. 2. The energy stored at the crack tip in the adhesive layer under external loads is directly related to the deformation of the adhesive layer at the crack tip, $\hat{w}$ in normal direction and $\hat{v}$ in tangential direction. The energy per unit crack area advance forms the energy release rate (ERR) in mode I and mode II for a single-layer adhesive joint, which are defined by

$$J_{\mathrm{I}}=\int_0^{\hat{w}}\sigma\,\mathrm{d}w\,,\qquad J_{\mathrm{II}}=\int_0^{\hat{v}}\tau\,\mathrm{d}v \qquad \text{(3a, b)}$$

and the total ERR is $J = J_{\mathrm{I}} + J_{\mathrm{II}}$. For linear elastic adhesives

$$J_{\mathrm{I}}=\frac{1}{2}\frac{\overline{E}}{t}\hat{w}^2\,,\qquad J_{\mathrm{II}}=\frac{1}{2}\frac{G}{t}\hat{v}^2 \qquad \text{(4a, b)}$$

These expressions are used by e.g. Fernlund and Spelt (1994) for strength analysis and by Wang and Rose (1997) to calculate the stress intensity factors K_{I} and K_{II}.

In the next chapter, the general solution of an unbalanced joint is given. The general solution to an unbalanced DCB-specimen is given in Chapter 3. The mixed mode effect due to material and geometry unbalances is studied by the B/A model. The final part of the paper deals with mixed mode testing of adhesive layer by an unsymmetric DCB-specimen.

2. Unbalanced joints

The general case of a single-layer adhesive joint is unbalanced, $E_1 t_1^2 \neq E_2 t_2^2$. In this case, from the governing equations (1a, b), two uncoupled differential equations in sixth and seventh order are derived as

$$\begin{cases} w^{IV}(x) - Cw^{VI}(x) + Bw''(x) - (BC - AD)w(x) = 0 \\ \left[v^{IV}(x) - Cv^{VI}(x) + Bv''(x) - (BC - AD)v(x) \right]'' = 0 \end{cases} \quad (5a, b)$$

where $B > 0$, $C > 0$ and $BC - AD > 0$. Both equations share the characteristic equation

$$r^6 - Cr^4 + Br^2 - (BC - AD) = 0 \quad (6)$$

which has six real roots

$$r_{1,2,3,4} = \pm\kappa_1 \pm i\kappa_2, \qquad r_{5,6} = \pm\kappa_3 \quad (7)$$

The roots can be calculated through, for example, Cardano's formula. Moreover, Eq. (5b) has an additional characteristic equation, with the root $r = 0$, which gives an extra constant term in the general solution for the shear deformation $v(x)$. Hence, the general solutions for the peel and shear deformations are

$$\begin{cases} w(x) = e^{\kappa_1 x}(\overline{K}_1 \sin\kappa_2 x + \overline{K}_2 \cos\kappa_2 x) + e^{-\kappa_1 x}(\overline{K}_3 \sin\kappa_2 x + \overline{K}_4 \cos\kappa_2 x) + \overline{K}_5 e^{\kappa_3 x} + \overline{K}_6 e^{-\kappa_3 x} \\ v(x) = e^{\kappa_1 x}(K_1 \sin\kappa_2 x + K_2 \cos\kappa_2 x) + e^{-\kappa_1 x}(K_3 \sin\kappa_2 x + K_4 \cos\kappa_2 x) + K_5 e^{\kappa_3 x} + K_6 e^{-\kappa_3 x} + K_7 \end{cases} \quad (8a, b)$$

where $\overline{K}_{1-6}$ and K_{1-7} are integration constants. In every trigonometric and exponential term, the wave numbers $\kappa_{1,2,3}$, appear together with x, the coordinate in the longitudinal direction of the overlap. These wave numbers, with dimension [length^{-1}], are just another representation form of the cross-sectional parameters, cf. Eq. (2). The appearance of $\kappa_{1,2,3}$ in the general solutions for both $w(x)$ and $v(x)$ interrelate the integration constants in Eq. (8). By differentiating the general solutions and re-entering them back into Eq. (1), the following six relationships between the integrations constant K_{1-6} and $\overline{K}_{1-6}$ are obtained

$$\begin{aligned} &\overline{K}_1 = \alpha_1 K_1 - \alpha_2 K_2, \quad \overline{K}_2 = \alpha_2 K_1 + \alpha_1 K_2, \quad \overline{K}_3 = -\alpha_1 K_3 - \alpha_2 K_4, \\ &\overline{K}_4 = \alpha_2 K_3 - \alpha_1 K_4, \quad \overline{K}_5 = \alpha_3 K_5, \quad \overline{K}_6 = -\alpha_3 K_6 \end{aligned} \quad (9a\text{-}f)$$

where

$$\alpha_1 = \frac{\kappa_1}{D}(C - \kappa_1^2 + 3\kappa_2^2), \ \alpha_2 = \frac{\kappa_2}{D}(C + \kappa_2^2 - 3\kappa_1^2), \quad \alpha_3 = \frac{\kappa_3}{D}(C - \kappa_3^2) \quad (10a, b, c)$$

Note that the parameters $\alpha_{1,2,3}$ are dimensionless and only depend on the cross-sectional parameters. Thus, the general solutions contain only seven independent integration constants, which are to be determined by seven boundary conditions, cf. Högberg (2004).

3. Unbalanced DCB-specimen

An unbalanced DCB-specimen with semi-infinite overlap is studied by use of the B/A model. Figure 2 shows the crack length a and the external peeling force F. The crack tip is situated at $x = 0$. Far from the crack tip, the stress and deformation in the adhesive layer fade out, which leads to seven integration constants being zero: $K_{1,2,5,7} = \overline{K}_{1,2,5} = 0$. The general solutions for the peel and shear deformations of the adhesive layer become

$$\begin{cases} w(x) = e^{-\kappa_1 x}(\overline{K}_3 \sin\kappa_2 x + \overline{K}_4 \cos\kappa_2 x) + \overline{K}_6 e^{-\kappa_3 x} \\ v(x) = e^{-\kappa_1 x}(K_3 \sin\kappa_2 x + K_4 \cos\kappa_2 x) + K_6 e^{-\kappa_3 x} \end{cases} \quad (11)$$

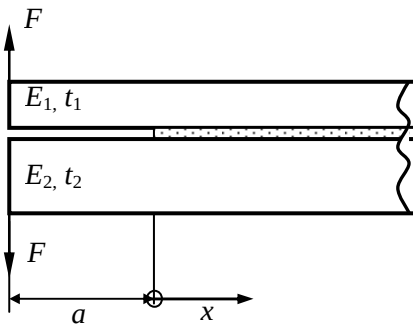

Figure 2 The unbalanced Double Cantilever Beam (DCB) specimen.

Observe that the six integration constants above are related to each other according to Eq. (9), which results in only three independent integration constants. Three boundary conditions can be obtained by the sectional forces at the crack tip. The sectional forces at $x = 0$ are

$$N_1 = N_2 = 0, \qquad V_1 = -V_2 = V = F, \qquad M_1 = -M_2 = M = Fa \tag{12a, b, c}$$

In the following analysis, the notation V and M are used instead of F and Fa for the forces. Equations (11) and (12) give an equation system consisting of the boundary conditions in matrix form as

$$\begin{bmatrix} \bar{\kappa}_2(1-\frac{g_1}{S_B}) & -\bar{\kappa}_1(1+\frac{g_1}{S_B}) & \bar{\kappa}_3^3\frac{g_3}{S_B} \\ -2\bar{\kappa}_1\bar{\kappa}_2\sqrt{C} & g_2\sqrt{C} & g_3\sqrt{C} \\ \bar{\kappa}_2 & -\bar{\kappa}_1 & -\bar{\kappa}_3 \end{bmatrix} \begin{bmatrix} K_3 \\ K_4 \\ K_6 \end{bmatrix} = \frac{tC}{b\bar{E}} S_D \begin{bmatrix} M \\ V \\ M \end{bmatrix} \tag{13}$$

where

$$g_1 = (\bar{\kappa}_1^2 + \bar{\kappa}_2^2)(2\bar{\kappa}_1^2 - 2\bar{\kappa}_2^2 - 1), \qquad g_2 = \bar{\kappa}_1^2 - \bar{\kappa}_2^2 - 1, \qquad g_3 = \bar{\kappa}_3^2 - 1 \tag{14a, b, c}$$

Except the cross-sectional parameter C, all other parameters in the 3x3 matrix on the left hand side are dimensionless. The parameters S_B, S_D and $\bar{\kappa}_{1,2,3}$ are dimensionless versions of B, D and $\kappa_{1,2,3}$. They are defined by

$$\bar{\kappa}_{1,2,3} = \frac{\kappa_{1,2,3}}{\sqrt{C}}, \qquad S_B = \frac{B}{C^2}, \qquad S_D = \frac{D}{C\sqrt{C}} \tag{15a, b, c}$$

The integration constants $K_{3,\,4,\,6}$ can be solved in closed form

$$\begin{aligned} K_3 &= -\frac{t\sqrt{C}}{b\bar{E}}\frac{S_D}{\bar{\kappa}_2 g}\left[g_{31}(\bar{\kappa}_1 V + g_2 M\sqrt{C}) + \bar{\kappa}_1 g_1(\bar{\kappa}_3 V + g_3 M\sqrt{C})\right] \\ K_4 &= -\frac{t\sqrt{C}}{b\bar{E}}\frac{S_D}{g}\left[g_{31}(V + 2\bar{\kappa}_1 M\sqrt{C}) - g_1(\bar{\kappa}_3 V + g_3 M\sqrt{C})\right] \\ K_6 &= -\frac{t\sqrt{C}}{b\bar{E}}\frac{S_D}{g} g_1\left[2\bar{\kappa}_1 V + g_{21} M\sqrt{C}\right] \end{aligned} \tag{16a, b, c}$$

where

$$\begin{aligned} &g_{21} = 3\bar{\kappa}_1^2 - \bar{\kappa}_2^2 - 1, \qquad g_{31} = \bar{\kappa}_3^3(\bar{\kappa}_3^2 - 1) + \bar{\kappa}_3 S_B, \\ &g = g_1(\bar{\kappa}_3 g_{21} - 2\bar{\kappa}_1 g_3) + g_{31}(2\bar{\kappa}_1^2 - g_2) \end{aligned} \tag{17a, b, c}$$

The remaining integration constants, $\bar{K}_{3,4,6}$, are given by Eq. (9). For a semi-infinite unbalanced DCB-specimen, the deformations of the adhesive layer in peel and in shear at the crack tip are

$$\hat{w} = w(0) = \bar{K}_4 + \bar{K}_6, \qquad \hat{v} = v(0) = K_4 + K_6 \tag{18a, b}$$

Together with Eq. (9), inserting the integration constants in Eq. (16) into Eq. (18), the deformation components become

$$\begin{cases} \hat{w} = -\dfrac{t\sqrt{C}}{b\bar{E}}\dfrac{S_D}{g}\left[g_{31}\left((\dfrac{\bar{\kappa}_1}{\bar{\kappa}_2}\alpha_2 - \alpha_1)V + (\dfrac{g_2}{\bar{\kappa}_2}\alpha_2 - 2\bar{\kappa}_1\alpha_1)M\sqrt{C} \right) + \right. \\ \qquad \left. + g_1\left((\bar{\kappa}_3(\dfrac{\bar{\kappa}_1}{\bar{\kappa}_2}\alpha_2 + \alpha_1) - 2\bar{\kappa}_1\alpha_3)V + (g_3(\dfrac{\bar{\kappa}_1}{\bar{\kappa}_2}\alpha_2 + \alpha_1) - g_{21}\alpha_3)M\sqrt{C} \right) \right] \\ \hat{v} = -\dfrac{t\sqrt{C}}{b\bar{E}}\dfrac{S_D}{g}\left[g_{31}(V + 2\bar{\kappa}_1 M\sqrt{C}) + g_1\left((2\bar{\kappa}_1 - \bar{\kappa}_3)V + (g_{21} - g_3)M\sqrt{C} \right) \right] \end{cases} \qquad (19a, b)$$

When the crack length a is large, the bending moment M dominates and $V \approx 0$, then

$$\begin{cases} \hat{w} = -\dfrac{MCt}{b\bar{E}}\dfrac{S_D}{g}\left[\dfrac{\alpha_2}{\bar{\kappa}_2}(g_2 g_{31} + \bar{\kappa}_1 g_1 g_3) + \alpha_1(g_1 g_3 - 2\bar{\kappa}_1 g_{31}) - \alpha_3 g_1 g_{21} \right] \\ \hat{v} = -\dfrac{MCt}{b\bar{E}}\dfrac{S_D}{g}\left[2\bar{\kappa}_1 g_{31} + g_1(g_{21} - g_3) \right] \end{cases} \qquad (20a, b)$$

The values of the deformations at the crack tip are compared to the results of FE-analyses in the sequel.

For the semi-infinite balanced DCB-specimen, i.e. $E_1 t_1^2 = E_2 t_2^2$ and if L is long, the peel and shear components of the deformation of the adhesive layer become

$$\begin{cases} w(x) = e^{-\kappa_p x}(S_3 \sin\kappa_p x + S_4 \cos\kappa_p x) \\ v(x) = S_6 e^{-\kappa_s x} \end{cases} \qquad (21a, b)$$

with the integration constants

$$\begin{aligned} S_3 &= -\frac{2\kappa_p^2 t}{b\bar{E}}M = -\frac{2\kappa_p^2 t}{b\bar{E}}Fa \\ S_4 &= \frac{2\kappa_p^2 t}{b\bar{E}}(\frac{V}{\kappa_p} + M) = \frac{2\kappa_p^2 t}{b\bar{E}}Fa(\frac{1}{\kappa_p a} + 1) \\ S_6 &= 0 \end{aligned} \qquad (22a, b, c)$$

where $\kappa_p^4 = B/4$ and $\kappa_s^2 = C$. The expressions to the left for S_3 and S_4 in Eq. (22) are valid for arbitrary loading of V and M; the expressions to the right are for the case $M = Va = Fa$. The adhesive layer deforms in pure mode I. Note that the adherends are not necessarily identical, the only requirement is that the relationship, $E_1 t_1^2 = E_2 t_2^2$, is fulfilled. The peel and shear components of the deformation of the adhesive layer at the crack tip are

$$\hat{w} = w(0) = S_4, \qquad \hat{v} = v(0) = 0 \qquad (23a, b)$$

The external loads on a DCB-specimen are self-balanced and the mode mixity is accomplished by introducing geometrical or material unbalances in the adherends. For elastic adhesives, the mode mixity is directly related to the deformations of the adhesive layer at the crack tip, $\hat{w}$ and $\hat{v}$ respectively, cf. Eq. (4). For different cases of DCB-specimens, $\hat{w}$ and $\hat{v}$ are given by Eqs. (19), (20) or (23). The peel and shear stress distributions in the adhesive layer can be obtained by using the linear elastic constitutive relationships, viz. $\sigma(x) = (\bar{E}/t)w(x)$ and $\tau(x) = (G/t)v(x)$, together with closed form solution of the peel and shear deformation distribution of the adhesive layer, $w(x)$ and $v(x)$ given by Eqs.(11) or (21).

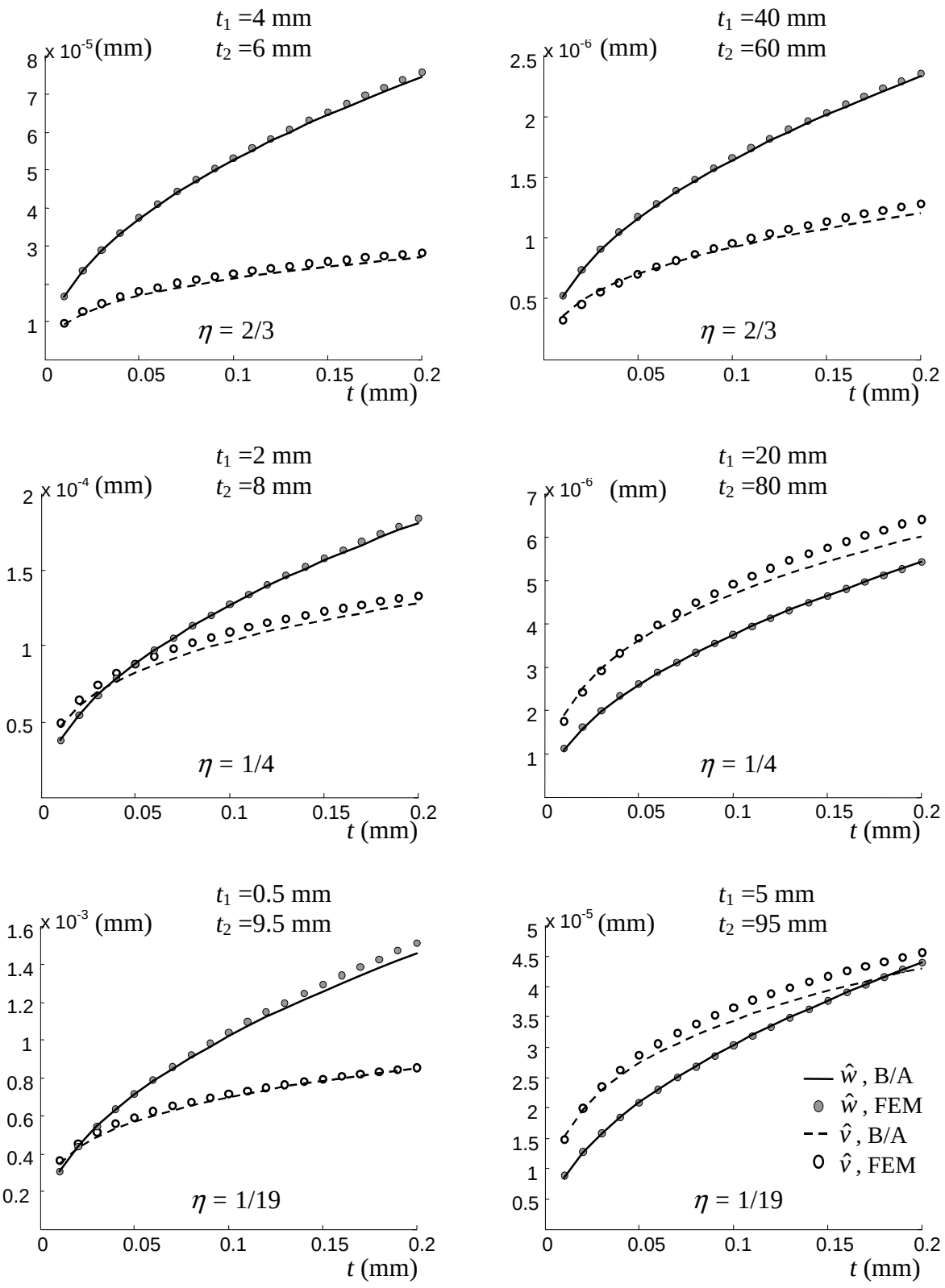

Figure 3 Effects of geometrical unbalance for a materially balanced DCB, as a function of the thickness of the adhesive layer, t = 0.01 – 0.2 mm. Six cases are studied. Comparison is made between the B/A model and continuum model by FE-analyses.

Unsymmetric DCB-specimens are materially balanced and geometrically unbalanced joints. Figure 3 shows the crack tip deformations with F = 10 N for six different cases of geometrical unbalance in the joints, i.e. the parameter $\eta = t_1/t_2$ varies. The B/A model is compared to FE-analysis with continuum elements. The common parameters used are

- The overlap length is L = 200 mm, the joint width b = 1 mm, the crack length a = 200 mm;
- The adherends are made of steel, with E_1 = 200 GPa, ν = 0.3;
- The adhesive is epoxy, with E = 2 GPa, ν = 0.4.

The three graphs in the left column show unsymmetric DCB-specimens with a total thickness of both adherends, $t_1 + t_2$ = 10 mm, while the three graphs in the right column have much thicker adherends, $t_1 + t_2$ = 100 mm. The thickness of the adhesive layer varies, t = 0.01 - 0.2 mm. Different degrees of unbalance in joint geometry are presented in three rows; $\eta = t_1/t_2$ = 2/3, 1/4, 1/19 in row one, two and three respectively. Good agreement is observed for the peel and the shear deformation for both models.

The deformation at the crack tip is much larger for geometrically more unbalanced joints. The peel deformation, $\hat{w}$, for the cases η = 1/19 (row three) is approximately eight times larger than the value for the cases η = 1/4 (row two). The shear deformation, $\hat{v}$, is approximately seven times larger. The peel deformation for the cases η = 1/4 (row two) is roughly twice the value for the cases η = 2/3 (row one) and the shear deformation five times larger. These ratios are nearly independent on the thickness of the adhesive layer, t, and the model used.

The deformation at the crack tip increases when the ratio of the thickness of the adhesive layer and the adherends, $t/(t_1+ t_2)$, increases. This is due to the overall stiffness of the joint decrease with a thicker adhesive layer. The deformation in mode I (peel) dominates in most cases for a DCB-specimen, the shear deformation only dominates in some extremely unbalanced cases.

The ERR for a semi-infinite unbalanced DCB-specimen is decomposed in mode I and II according to Eq. (4), where the deformations at the crack tip are given by Eqs. (18-20). For a balanced DCB-specimen, the ERR's become

$$J_{\mathrm{I}} = 6\left(\frac{1}{E_1 t_1^3} + \frac{1}{E_2 t_2^3}\right)\left(\frac{Fa}{b}\right)^2\left(\frac{1}{\kappa_{\mathrm{p}} a} + 1\right)^2, \qquad J_{\mathrm{II}} = 0 \tag{24a, b}$$

If the crack length a is long, $1/(\kappa_{\mathrm{p}} a) \to 0$, J_{I} in Eq. (24a) is independent on the properties of the adhesive.

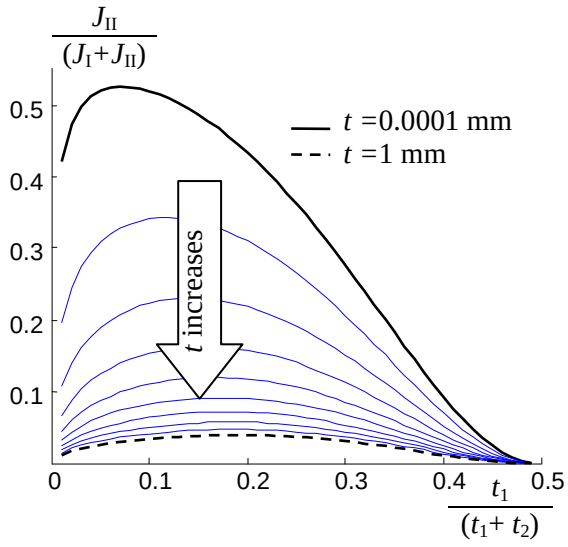

Figure 4 Mode mixity of an unsymmetrical DCB-specimen due to geometrical unbalance. The B/A model is applied and $t_1/(t_1+t_2)$ = 0 - 0.5 mm.

Figure 4 illustrates the mode mixity due to geometrical unbalance for an unsymmetric DCB-specimen. The total thickness of both adherends remains constant, $t_1 + t_2 = 10$ mm. Other parameters are the same as above. Each curve in the graph shows a specific thickness in the adhesive layer, the thinnest is at the top with $t = 0.1$ μm. The adhesive layer increase in thickness incrementally according to $t = i^4 \cdot 0.1$ μm (i =1-10) for each curve beneath, until t reaches 1 mm when it comes to the dashed line at the bottom of the graph. For joints with a very thin adhesive layer, a quite large range of mode mixity can be achieved. Pure mode I is achieved when the adherends are balanced or when one adherend is virtually zero in thickness. Pure mode II can not be attained with a DCB-specimen.

4. Mixed mode testing of adhesive layer

To obtain the constitutive behaviour of adhesive layers, an inverse method is employed in experimental studies by e.g. Andersson and Stigh (2004), Leffler et al. (2006) and Högberg and Stigh (2006). This method is based on the energetic balance of a specimen by the use of the J-integral. For an elastic adhesive joint, linear or nonlinear, the J-integral is defined by

$$J = \int_s \left(W \mathrm{d}y - \mathbf{T} \cdot \frac{\mathrm{d}\mathbf{u}}{\mathrm{d}x} \mathrm{d}s\right) \tag{25}$$

where $W = \int \boldsymbol{\sigma}\, \mathrm{d}\boldsymbol{\varepsilon}$ is the strain energy density, cf. Rice (1968). The traction vector $\mathbf{T} = \boldsymbol{\sigma}\mathbf{n}$, where $\boldsymbol{\sigma}$ is the stress tensor and $\mathbf{n}$ the outwards unit vector normal to the counter-clockwise integration path s. The deformation vector and the strain tensor are denoted as $\mathbf{u}$ and $\boldsymbol{\varepsilon}$, respectively. The coordinate system is defined in Fig. 5.

The ERR of the adhesive joint can be determined by the J-integral if a closed integration path without singularity is chosen, e.g. the path s shown in Fig. 5 for the UDCB-specimen. The parts of the path that are not traction-free are situated at the crack tip region and the loading point area. The J-integral along the closed integration path s, or path AB and BA, yields energetic force equilibrium

$$J = J_{\mathrm{AB}} + J_{\mathrm{BA}} = 0 \tag{26}$$

We first focus on the path AB, which goes through the adhesive layer at the crack tip. The adhesive layer deforms in a combination of two modes: peel (mode I) and shear (mode II). Evaluating the terms in Eq. (25) gives

$$J_{\mathrm{AB}} = \int_0^v \tau \, \mathrm{d}\tilde{v} + \int_0^w \sigma \, \mathrm{d}\tilde{w} \tag{27}$$

where τ and σ are the tangential and normal components of the traction vector, and v and w are the tangential and normal deformation of the adhesive layer through the path AB. This expression is equivalent to Eq. (3), which is defined as the potential to the cohesive relation of the adhesive. On the path BA, only the vertical paths under the loading points, at $x = -a$, contribute to J_{BA}. Assuming the adherends to deform according to Euler-Bernoulli beam theory, Eq. (25) yields the total ERR due to the load

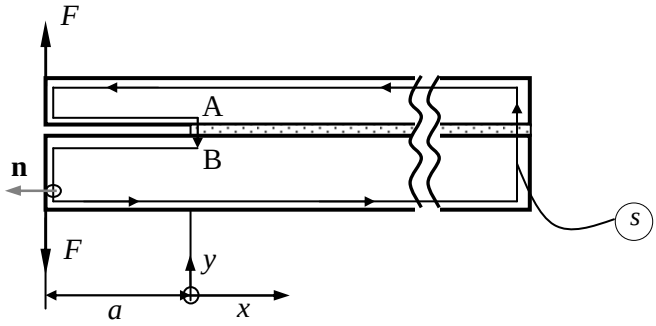

Figure 5 Integration path s on the UDCB-specimen.

$$-J_{BA} = \frac{F}{b}(w_1' - w_2') \tag{28}$$

where b is the width of the specimen and $w_{1,2}'$ is the rotation of the adherends at the loading point. The ERR due to the load, Eq. (28), balances the ERR on the adhesive layer, Eq. (27), by Eq. (26). All parameters on the right hand side of Eq. (28) are measurable during the experiment, which enables the evaluation of the constitutive behaviour of the adhesive layer in term of stress-deformation relationships by

$$\sigma(w,v) = \frac{\partial J_{AB}}{\partial w}, \qquad \tau(w,v) = \frac{\partial J_{AB}}{\partial v} \tag{29a, b}$$

The J-integral is valid for elastic material and for any elastoplastic material under monotonic and proportional loading. The ERR due to the load, Eq. (28) is dependent on the specimen configuration. However, the ERR through the adhesive layer, Eq. (27), is not dependent on the specimen configuration.

The theory for obtaining the constitutive behaviour of the adhesive layer sets more requirements on the UDCB-geometry:

1. In order to be able to treat the adhesive layer as a continuous distribution of bi-directional springs, the adhesive layer should be thin and flexible in comparison with the adherends. This requirement sets a condition on the relative stiffness of the adherends as compared to the adhesive as $(E_1 t)/(\overline{E}\, t_1) > 0.1$, which is an essential criterion to validate the B/A model, cf. Högberg (2004).
2. The B/A model is based on small deformations. Thus a requirement is that the deformation of the adhesive layer at the crack tip is small in comparison with the overall dimensions of the joint.
3. The overlap length should be long since the specimen is considered as semi-infinite in the derivation of Eq. (28). The condition, $\kappa_{1,2,3} L > 3$, should be fulfilled, cf. Högberg (2004).
4. The adherends should deform linear elastically. The maximum bending moment in an adherend occurs near the crack tip, its magnitude is close to the bending moment at the crack tip. Thus, the maximum stress in the adherends at $x = 0$ should be smaller than the yield strength of the adherends, i.e. $\sigma_{max} = (6Fa)/(bt_1^{\,2}) < \sigma_{yield}$.

The material choice is the same as for the mode I experiment performed with the DCB-specimen by Andersson and Stigh (2004) and the mode II experiment performed with the ENF-specimen by Leffler et al. (2006). The adhesive, DOW Betamate XW1044-3, is a toughened epoxy, with E = 2 GPa and v = 0.4. The adherends are made of tool steel, with E_1 = 200 GPa, v = 0.3 and σ_{yield} = 500 MPa. With these chosen materials, the following dimension of the UDCB-specimen satisfies all requirements given above

Overall joint:	L = 100 mm, b = 4 mm, a = 50 mm
Adhesive:	t = 0.2 mm
Adherends:	t_1 = 2 mm, t_2 = 2, 4, …12 mm

Simulation of the UDCB-specimen are performed using the commercial FE-program ABAQUS (v6.4). The adherends are modelled as Euler-Bernoulli beams and the adhesive layer is modelled by interphase elements developed by Salomonsson (2002). The constitutive behaviour of the adhesive layer is given by the mixed mode cohesive law given by Högberg (2006). The simulations are performed using a prescribed displacement on the loading points. Figure 6 shows the reaction force, F, and the ERR due to F, J_{BA}, cf. Eq. (28). The loading system is stable, F declines somewhat after reaching the peak value. The ERR, J_{BA}, increases until the fracture energy is reached as a plateau. When both adherends are equal in thickness, the adhesive layer deforms in pure mode I. An increasing t_2 causes an increase in mode II loading of the adhesive layer. The proportion of the mode II deformations is slightly larger when the adhesive behaves linearly elastic. However, for all chosen t_2, the adhesive mainly deforms in mode I; the pure mode II case cannot be achieved with the DCB-specimen.

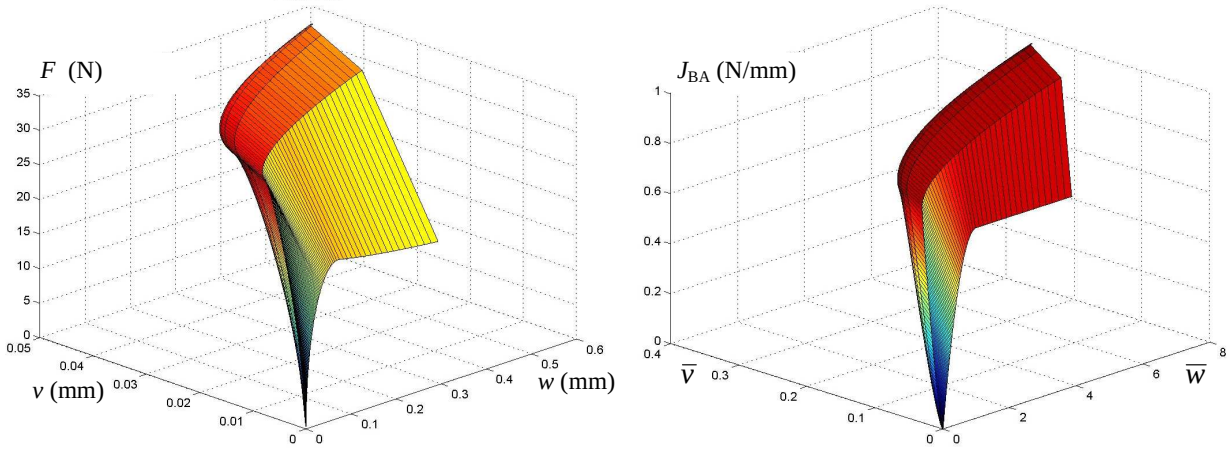

Figure 6 Simulation results on the UDCB-specimen, $F(w,v)$ and $J(\bar{w},\bar{v})$, where $\bar{w}$ and $\bar{v}$ are normalised by the critical deformations obtained from the mode I and the mode II experiments.

6. Conclusion

The mechanical and fracture properties of the adhesively bonded unbalanced Double Cantilever Beam (DCB) specimen are studied. The deformation distribution of the adhesive layer is given for different cases of DCB-specimen. For semi-infinite DCB-specimens, the energy release rate (ERR) is directly related to the deformation of the elastic adhesive layer at the crack tip. Thus, the mode I and II components of the ERR can be instantly evaluated by the peel and shear deformation respectively. The unbalance in the adherends causes mixed mode loading on the adhesive layer. This effect is analysed by the B/A model, which is compared to the continuum model in FE-analysis and good agreement is shown. For experimental testing of adhesive layer under mixed mode loading, unsymmetric DCB-specimens are dimensioned based on the applicability of the *J*-integral.

Acknowledgement:

The presented work is a part of co-operation project with the Mechanics of Material group at the Department of Applied Mechanics at Chalmers University of Technology. The author would like to acknowledge Kent Salomonsson, Division of Mechanics of Materials at University of Skövde, for cooperation with the FE-simulations.

References:

Andersson T. and Stigh U. (2004) The stress-elongation relation for an adhesive layer loaded in peel using equilibrium of energetic forces. International Journal of Solids and Structures 41, 413-434.

Fernlund G. and Spelt J.K. Mixed mode energy release rate for adhesively bonded beam specimen. Journal of Composites Technology and Research 1994; 16(3): 234-243.

Högberg J.L. (2004) Mechanical behaviour of single-layer adhesive joints – an integrated approach. Thesis for the degree of Licentiate of Engineering, Chalmers University of Technology, Göteborg, Sweden. ISSN 1650-8912 2004:3. (Available at *www.his.se/MechMat*)

Högberg J.L. and Stigh U. (2006) Specimen proposals for mixed mode testing of adhesive layer. Engineering Fracture Mechanics 73, 2541-2556.

Högberg J.L. (2006) Mixed mode cohesive law. Accepted for publication in International Journal of Fracture.

Klarbring A. (1991) Derivation of a model of adhesively bonded joints by the asymptotic expansion method. International Journal of Engineering Science 29, 493-512.

Leffler K., Alfredsson K.S. and Stigh U. (2006) Shear behaviour of adhesive layers. To appear in International Journal of Solids and Structures.

Rice J.R. (1968) A path independent integral and the approximate analysis of strain concentration by notches and cracks. Journal of Applied Mechanics 35, 379-386.
Salomonsson K. (2002) Interphase elements connection structural finite elements formulation, implementation and verification. Master thesis. Chalmers University of Technology, Göteborg, Sweden. (Available at *www.his.se/MechMat*)
Wang C.H. and Rose L.R.F. (1997) Failure analysis of adhesively bonded joints. Advances in Fracture Research – Proceedings of ICF9. Karihaloo B.L. et al. Pergamon, Amsterdam: 3057-3064.